On the scaling of thermal stresses in passivated nanointerconnects

P. Sharma[a)]
Department of Mechanical Engineering, University of Houston, Houston, Texas 77204

S. Ganti
Advanced Mechanical Technologies, General Electric Global Research Center, Niskayuna, New York 12309

H. Ardebili
Micro and Nanostructures Technology, General Electric Global Research Center, Niskayuna, New York 12309

A. Alizadeh
Polymers and Specialty Chemicals Technology, General Electric Global Research Center, Niskayuna, New York 12309

(Received 24 July 2003; accepted 19 October 2003)

Much work has been done in the approximation of the stress state of microelectronic interconnects on chips. The thermally induced stresses in passivated interconnects are of interest as they are used as input in interconnect reliability failure models (stress-driven void growth, electromigration-driven void growth). The classical continuum mechanics and physics typically used is, however, intrinsically size independent. This is in contradiction to the physical fact that at the size scale of a few nanometers, the elastic state is size dependent and a departure from classical mechanics is expected. In this work, we address the various physical causes (and the affiliated mathematical modeling) of the size dependency of mechanical stresses in nanointerconnects. In essence, we present scaling laws for mechanical stresses valid for nanosized interconnects. © *2004 American Institute of Physics.* [DOI: 10.1063/1.1632011]

I. INTRODUCTION

The technological importance of assessing the reliability of conventional microelectronic interconnects can hardly be overemphasized. One of the important failure modes in electronic systems and also a major impediment to the development of miniaturized electronics is the mechanical failure of interconnects during fabrication and operation.[1–7] A schematic of a typical passivated interconnect is shown in Fig. 1. The passivation process, whereby a dielectric oxide layer is deposited on the interconnect structure, is necessary both for the proper functioning of several devices as well as for environmental protection. Passivation is typically accomplished at high temperatures (~400 °C). Due to thermal expansion mismatch between the various constituents of the electronic system, subsequent cooling to operational temperatures (~25 °C) leads to the development of residual stresses in interconnects. These mechanical stresses generated during the fabrication process (and modified in the subsequent operational electrical and thermal environment) are then responsible for the eventual nucleation, evolution, and coalescence of voids. The final void coalescence, when spread across the thickness of the interconnect, causes complete mechanical failure (and often catastrophic electrical failure) (e.g., Refs. 8 and 9 and references therein). This problem is exacerbated by technology-driven reduction in interconnect and chip feature sizes. It is worth recalling that the various electronic industry roadmaps (e.g., the ''International Technical Roadmap for Semiconductors'' [10]) have forecast interconnect sizes of 20–30 nm by the year 2009. Considering the rapid advances being made in nanowire technology for use in nanoelectronics,[11] the scaling of mechanical stresses in nanointerconnects (and hence their reliability) is of crucial importance. The scaling of mechanical stresses as the interconnect dimensions shrink also has important implications for the continued validity of the so-called Moore's law.[12] Worth noting is that size effects in interconnects at less than 65 nm and the consequent impact on reliability are considered to be one of the key technological challenges.[10] Kaloyeros *et al.*[13] provide an interesting perspective on the use of nanotechnology for nanointerconnects.

Clearly, mechanical stresses are only one of the several issues that need to be addressed in regard to nanointerconnects. Other aspects that may be as important as or even more important than mechanical stresses are electromigration, dimensional control of processing/fabricating interconnects at the nanoscale, electrical design issues, suitable low-k dielectric materials, etc. For further information and discussion, see, for example, Pang *et al.*[14] This work is limited in its scope; only scaling of mechanical stresses for nanointerconnects is addressed. With the current lack of such a scaling model, one can only speculate about the nature of stresses in nanointerconnects. Will they increase dramatically so as to override and cause the early demise of Moore's law or decrease sufficiently to exclude mechanical stresses from the list of reliability concerns? Perhaps the change in mechanical stresses in the nanointerconnects would be insignificant so

[a)]Author to whom correspondence should be addressed; electronic mail: psharma@uh.edu

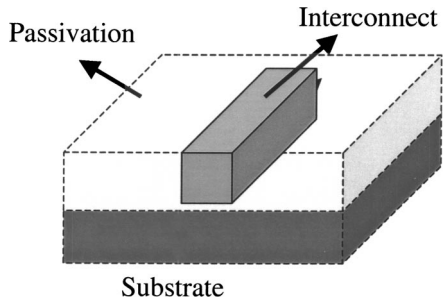

FIG. 1. Schematic of a passivated interconnect on chip.

that classical mechanics may continue to be used at such small length scales, and attention to the scaling of other (aforementioned) nanointerconnect related issues must then be intensified. The present work, based on theoretical considerations, attempts to provide answers to such questions and speculations.

While a tremendous amount of work (within the context of classical continuum mechanics) has been done on assessing the mechanical stress state as well as the reliability of on-chip interconnects in the past two decades, the scaling of stresses in nanointerconnects (which requires incorporation of size effects) has not been addressed yet. This limitation of existing literature pertains to both detailed numerical simulations[1–3] as well as to approximate analytical models.[4–7] In short, all existing models will predict the same stress state regardless of the absolute size of the interconnect (as long as it is scaled larger or smaller in a self-similar fashion). The size independence of classical mechanics (and by extension all previous work) is in contradiction to the physical fact that, at the size scale of a few nanometers, deformations and elastic states are size dependent, and a qualitative departure from classical mechanics is expected (of course, the relevant question then is how great is this departure for interconnects of the size of, say, 20–30 nm?). While it is clearly possible that once all necessary scaling laws have been established classical mechanics may turn out to be not so bad an approximation, such a conclusion (or the lack of it) cannot be reached via classical continuum mechanics models.

Even though all existing work on interconnect stress and reliability estimation is size independent and hence inappropriate for extension to nanointerconnects, to establish the appropriate context, a brief review of the representative existing work on the estimation of stresses in microinterconnects is provided below.

Some of the earliest work on stress determination in passivated electronic interconnects is due to Niwa *et al.*,[5] Kato *et al.*,[15] and Korhonen *et al.*[4] While the last work was important in its discussion of various stress generation and relaxation mechanisms, the first two are often cited for their analytical model. References 5 and 15 employed Eshelby's treatment[16] of an embedded inclusion in an infinite elastic matrix to formulate their closed-form model. In their model, the interconnect is a circular/elliptical cylindrical inclusion embedded in an ''infinite amount'' of passivation material while subjected to a thermal mismatch eigenstrain. The last assumption allowed them an almost direct use of Eshelby's solution of an embedded inclusion containing a stress-free eigenstrain located in an infinite elastic medium. Subsequently, their model was improved by various researchers, e.g., Korhonen *et al.*[4] distinguished between the interconnect and passivation elastic constants. Among some recent work, Wikstrom *et al.*[1] presented a simple approach to approximate volume-averaged stresses. Their model is applicable only for a certain range of interconnect aspect ratios. Sharma *et al.*[6] made an improvement to the Niwa *et al.* model[5] by relaxing the restriction that the interconnect is surrounded by an infinite amount of passivation. In reality, the free surface of the passivation is often in close proximity to the interconnect, which can alter some aspects of the stress distribution. The work of Sharma *et al.*[6] employs the solution of an inclusion in half space (using an ''image force'' type analysis) to take this feature into account. More recently, a shear-lag type approach was adopted by Hsueh,[7] who presents a fairly comprehensive model of the stress state in rectangular passivated interconnects.

In the present work, we systematically track the two main physical causes of the size dependency of elasticity at the nanoscale. Based upon the postulated physical mechanisms of the elastic-state size dependency, we present (approximate) closed-form models for the stress state of nanointerconnects. In Sec. II, the two main physical causes of the size dependency of the elastic state are discussed. Based on the proposed physical mechanisms, an appropriate mathematical framework is developed for the analysis of a passivated metal interconnect. Numerical results and discussion are relegated to Sec. III. Of considerable importance are the limitations of this work. Those are also discussed in Sec. III. Closure is provided in Sec. IV.

II. SCALING LAWS FOR MECHANICAL STRESSES VALID FOR NANOSIZED INTERCONNECTS

Within the framework of formulating a size-dependent field theoretic modification of continuum theory valid at the nanoscale, we postulate two main causes of size dependency in elasticity.

(a) Interface/surface effects. For structures with sizes greater than 50 nm, typically, the surface-to-volume ratio is negligible and the deformation behavior is governed by classical bulk strain energy. However, at submicrometer inclusion (interconnect) length scales, the properties of the inclusion surface/interface are expected to play a role in the determination of the nanoinclusion (nanointerconnect) elastic state. This increasing role of surface or interface elasticity at smaller length scales induces a size effect in the otherwise classical size-independent elastic solutions.

(b) Nonlocal interactions. Classical elasticity is essentially a local theory and thus is considered to be valid only in the ''long'' wavelength limit. Each material point in the continuum theory represents the smeared or coarse-grained deformation behavior of its micro- (or more appropriately nano)constituents. This coarse-grained behavior of a suitably large, statistically representative number of atoms and grains is represented by the usual bulk elastic constants of the material. At length scales where the discrete nature of matter

becomes apparent, additional physical phenomena not readily included in the classical continuum mechanics framework become important. The typical coarse-graining implicit in the use of classic elastic constants becomes inadequate. Thus, on physical grounds, one can conceive that, at the size scale of a few nanometers, molecular interactions are increasingly nonlocal, thus violating the coarse-grained classic elastic assumption of locality. Simply put, stress-strain at a point at the nanoscale should depend on the elastic state of all surrounding neighborhood points rather than the state just at that point (as assumed by classical elasticity).

A. Derivation of stresses at the nanoscale: Interface effects

It should be pointed out that the physical mechanisms discussed in the preceding section hardly operate independently. It is convenient, however, to first address the two mechanisms separately and combine them later. This will facilitate qualitative understanding of each physical mechanism.

A generic and mathematical exposition on surface/interface elasticity has been presented by Gurtin and co-workers.[17–19] The interface/surface stress tensor $\boldsymbol{\sigma}^S$ is related to the deformation-dependent surface energy $\Gamma(\varepsilon_{\alpha\beta})$ by

$$\boldsymbol{\sigma}^S = \tau_0 \boldsymbol{\delta} + \frac{\partial \Gamma}{\partial \boldsymbol{\varepsilon}}. \tag{1}$$

Here, $\boldsymbol{\varepsilon}$ is the 2×2 strain tensor for surfaces, $\boldsymbol{\delta}$ represents the Kronecker delta for surfaces, while τ_0 is the deformation-independent surface/interfacial tension. Both boldfaced and index notation will be used as convenient. Note that the concepts of surface tension, surface stress, and surface energy are often confused and used interchangeably. Only for liquids are all three the same. For solids, they are vastly different and must be carefully distinguished. See, for example, the excellent review article by Ibach.[20] Isotropic behavior is assumed throughout. In the bulk of the material (i.e., within both the interconnect and the host passivation material but not on the interface), the equilibrium and constitutive equations of infinitesimal classical elastostatics without body forces are satisfied:

$$\operatorname{div} \boldsymbol{\sigma}^B = 0, \tag{2a}$$

$$\boldsymbol{\sigma}^B = \lambda \mathbf{I}^3 \operatorname{Tr}(\boldsymbol{\varepsilon}) + 2\mu\varepsilon, \tag{2b}$$

Where applicable, superscripts B and S indicate bulk and surface, respectively. At the interface, the concept of surface or interface elasticity[17–19] is introduced, which is missing from the classical elasticity formulation:

$$[\boldsymbol{\sigma}^B \cdot \mathbf{n}] + \operatorname{div}_s \boldsymbol{\sigma}^S = 0, \tag{3a}$$

$$\boldsymbol{\sigma}^B : (\mathbf{n} \otimes \mathbf{n}) = \boldsymbol{\sigma}^S : \boldsymbol{\kappa}, \tag{3b}$$

$$\boldsymbol{\sigma}^S = \tau^0 \mathbf{I}^2 + 2(\mu^S - \tau^0)\boldsymbol{\varepsilon}^S + (\lambda^S + \tau^0)\operatorname{Tr}(\varepsilon^S)\mathbf{I}^2. \tag{3c}$$

Here, λ and μ are the Lamé constants for the isotropic bulk material. Isotropic interfaces or surfaces can be characterized by surface Lamé constants λ^S, μ^S. Square brackets indicate a jump across the interface. Here, $\boldsymbol{\kappa}$ represents the second-rank curvature tensor of the surface/interface, and $\mathbf{n}$ is the normal vector on the interface. It is to be noted that only certain strain components appear within the constitutive law for surfaces due to the 2×2 nature of the surface stress tensor (i.e., strains normal to the surface are excluded). Thus, $\mathbf{I}^2$ represents the 2×2 identity tensor while $\mathbf{I}^3$ represents the same for the bulk second-rank tensor. Tr indicates the trace operation. In the absence of surface terms, Eqs. (3) reduce to the usual normal traction continuity equations of classical elasticity. div_s indicates the surface divergence.[17]

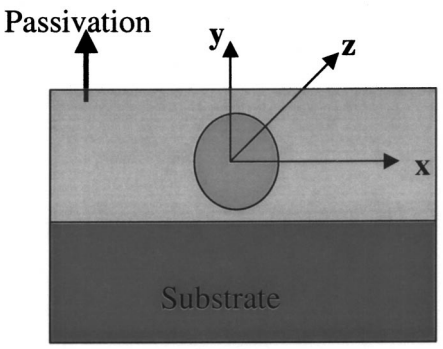

FIG. 2. Idealized schematic of the interconnect structure.

For simplicity and to avoid confounding the nanoscale physics with second-order effects, we shall assume that the interconnect is located in an infinite amount of passivation. This assumption is similar to that used in previous analytical work.[4,5] Unlike the former and like the latter work, we will take into account the differing elastic constants of the passivation and interconnect. Consider now a cylindrical interconnect of radius R_0, located in a passivation matrix and undergoing a dilatation eigenstrain, i.e., thermal expansion mismatch strain $\varepsilon^*_{11} = \varepsilon^*_{22} = \varepsilon^*_{33} = \varepsilon^* = \Delta\alpha\Delta T$, where $\Delta\alpha$ is the difference in the thermal expansion coefficients of the passivation and interconnect while T indicates temperature. The idealized geometry of a cylindrical interconnect is shown in Fig. 2. Note, however, that if one is to assume future application of nanowires as interconnects, the cylindrical structure (adopted for computational simplification in the current work) is exactly representative.

Recently, Sharma and Ganti[21] derived the general size-dependent Eshelby tensor for inclusions in the context of coupled bulk-surface elasticity. Some salient features of that derivation (adapted for our geometry) are reproduced here. Consider for the moment that the passivation and interconnect have the same elastic modulus although a thermal mismatch strain is prescribed in the region of the interconnect. The constraint on the elastic modulus will be removed later. We can write the constitutive equation in the interconnect-passivation systems as follows:

$$\boldsymbol{\sigma} = \mathbf{C} : \{\boldsymbol{\varepsilon} - \boldsymbol{\varepsilon}^* H(x)\}. \tag{4}$$

Here H is the Heaviside function and $\mathbf{C}$ is the stiffness tensor. Taking the divergence of Eq. (4), we obtain

$$\nabla \cdot \boldsymbol{\sigma} = \nabla \cdot (\mathbf{C} : \boldsymbol{\varepsilon}) - \nabla \cdot \{\mathbf{C} : \boldsymbol{\varepsilon}^* H(x)\} + [\boldsymbol{\sigma} \cdot \mathbf{n}] = \mathbf{0}, \tag{5}$$

where $\mathbf{n}$ is the normal vector on the interconnect-passivation interface and the square brackets indicate the jump across the

interface. It can be readily seen that the thermal mismatch strain term in Eq. (5) appears as a body force. Note that in classical elasticity the last expression in Eq. (5) is typically omitted since the jump in the normal tractions is zero. However, taking cognizance of Eq. (3a), i.e., coupling interface elasticity with bulk elasticity, we must rewrite Eq. (5) as

$$\boldsymbol{\nabla}\cdot\boldsymbol{\sigma}=\boldsymbol{\nabla}\cdot(\mathbf{C}:\boldsymbol{\varepsilon})-\underbrace{\boldsymbol{\nabla}\cdot\{\mathbf{C}:\boldsymbol{\varepsilon}^{*}H(x)\}+\mathrm{div}_{S}\,\boldsymbol{\sigma}^{S}}=\mathbf{0}. \quad (6)$$

The underlined term represents the body force from which the modified Eshelby tensor can be derived via the elastic Green's function after some algebra and integration.[20] The modified Eshelby tensor is then given implicitly by (for cylindrical geometry)

$$\boldsymbol{\varepsilon}=\mathbf{S}:\boldsymbol{\varepsilon}^{*}-\frac{\tau^{0}}{R_{0}K'}\mathbf{S}:\mathbf{I}-\frac{K^{S}}{R_{0}K''}(\mathbf{S}:\mathbf{I})\mathrm{Tr}(\mathbf{P}^{S}\boldsymbol{\varepsilon}\mathbf{P}^{S}),$$
$$\mathbf{P}^{S}=\mathbf{1}-\mathbf{n}\otimes\mathbf{n}. \quad (7)$$

Here $\mathbf{S}$ is the *classical* Eshelby tensor[16] for cylindrical geometry. ε is the actual strain developed in the interconnect due to the prescribed thermal mismatch. The tensor $\mathbf{P}^{S}$ is merely a projection tensor introduced by Gurtin and Murdoch.[18] Here K^{S} is a combination of surface elastic constants ($K^{S}=2\mu^{S}+\lambda^{S}$) while K' is $2\mu+2\lambda$ and K'' is $4\mu+2\lambda$. Due to the fact that the modified size-dependent Eshelby tensor is also uniform for the cylindrical geometry (like the classical one), one can then easily employ the Eshelby equivalent inclusion method[16] to take into account the difference in the elastic stiffness tensors of interconnect and passivation material (see also Korhonen *et al.*[4]). Finally, after employing Eq. (7), and the equivalent inclusion principle, size-dependent stresses within the interconnect can be written simply as

$$\sigma_{rr}=2(\mu_{I}+\lambda_{I})\frac{-2\mu_{P}\varepsilon^{*}-K^{S}\varepsilon^{*}/R_{0}-\tau_{0}/R_{0}}{2(\mu_{P}+\mu_{I}+\lambda_{I})+K^{S}/R_{0}} \quad (8)$$

Here, the subscript P refers to passivation and I to interconnect. Note that the interfacial elasticity effects enter the equations via K^{S} and τ_{0} weighted appropriately by the curvature $(1/R_{0})$ of the inhomogeneity. This makes the stress dependent upon the absolute size of the interconnect. Clearly, for ''large'' interconnect size (i.e., micrometer size), the impact of surface energies will disappear, degenerating to classical stresses (see, e.g., Niwa *et al.*[5] for this idealized structure). The evaluation of these interface energy and elasticity constants is discussed in Appendix A.

B. Derivation of stresses at the nanoscale: Nonlocal interactions

The various nonlocal interactions prevalent at the nanoscale may be mimicked phenomenologically via the nonlocal theory of elasticity. In fact the early attempts at formulating nonlocal constitutive laws were based on lattice dynamics.[23,24] Subsequently, rigorous theories of nonlocal continuum mechanics theories were proposed in several works.[24–26] Most of the literature in nonlocal interactions has been well summarized recently by Eringen.[27] The work of Reid and Gooding[28] should also be cited, they discuss a nonlocal inclusion (where the matrix and inclusion have same material properties). The latter (with minor modifications) will be useful in this work as it can be suitably combined with our derivation in the preceding section to address the nanointerconnect problem. The inclusion problem within the three-dimensional context has also been recently addressed in the work of Sharma and Ganti.[29]

In the nonlocal theory, the constitutive relations of classical elasticity are replaced by integral equations that are a function of all neighborhood points. A weaker form of the nonlocal representation can also be formulated whereby the stress tensor depends upon the gradients of the strains (accomplished through suitable series expansion of the nonlocal integral kernel in the Fourier domain; see Eringen[27]). The latter form, being analytically more tractable, is adopted in this work. In particular, we adopt the formalism of Reid and Gooding,[28] who correct the classical elasticity Lagrangian by adding suitable gradient terms. Thus, in the presence of gradient terms (for our cylindrically symmetric problem), the part of the Lagrangian that contributes to the field equations can be written as

$$\Psi_{\Lambda}^{\mathrm{gradient}}=\frac{1}{2}\lambda_{\Lambda}[\mathrm{Tr}(\boldsymbol{\varepsilon})]^{2}+\mu_{\Lambda}\boldsymbol{\varepsilon}:\boldsymbol{\varepsilon}+d\boldsymbol{\xi}:\boldsymbol{\xi}$$
$$-2(\lambda_{\Lambda}+\mu_{\Lambda})\varepsilon^{*}\mathrm{Tr}(\boldsymbol{\varepsilon})], \quad (9a)$$
$$\xi_{ijk}=(\varepsilon_{ij,k}+\varepsilon_{ik,j}-\varepsilon_{kj,i}). \quad (9b)$$

Here d is a phenomenological elastic parameter that represents the strength of the nonlocal interactions. It can be determined either by *ab initio* simulations or through suitable interpretation of phonon-dispersion curves (see Appendix B).

The cylindrically symmetric problem admits a displacement field that is radially symmetric, i.e., $u=u(r)$. The corresponding infinitesimal strain components in cylindrical polar basis are

$$\varepsilon_{rr}=\frac{\partial u}{\partial r},\quad \varepsilon_{\theta\theta}=\frac{u}{r},\quad \varepsilon_{zz}=0,\quad \varepsilon_{\theta\theta}^{S}=\frac{u}{R_{0}},\quad \varepsilon_{rr}^{S}=\varepsilon_{zz}^{S}=0. \quad (10)$$

Substituting Eq. (10) in Eq. (9), using the constitutive Eqs. (2) and (3), and taking the variation of the total energy with respect to the displacement fields, we obtain the governing field equation for gradient elasticity[28]

$$\frac{\partial^{4}u}{\partial r^{4}}+\frac{2}{r}\frac{\partial^{3}u}{\partial r^{3}}-\left[q^{2}+\frac{3}{r^{2}}\right]\frac{\partial^{2}u}{\partial r^{2}}-\left[\frac{q^{2}}{r}-\frac{3}{r^{3}}\right]\frac{\partial u}{\partial r}$$
$$+\left[\frac{q^{2}}{r^{2}}-\frac{3}{r^{4}}\right]u=0,$$
$$q=\sqrt{\frac{\lambda+2\mu}{2d}} \quad (11)$$

The general solution can then be written as

$$u(r)=\begin{cases}a(qr)+b(qr)^{-1}+cI_{1}(qr)+dK_{1}(qr), & r\leqslant R_{0},\\ e(qr)+f(qr)^{-1}+gI_{1}(qr)+hK_{1}(qr), & r>R_{0},\end{cases} \quad (12)$$

TABLE I. Estimation of material properties.

Parameter	SiO_2	Cu	Cu-SiO_2 interface
λ (MPa)	14.48	63.46	—
μ (MPa)	30.77	42.3	—
τ_0 (N/m)	—	—	1.5 (Cui *et al.* Ref. 29)
λ_S (N/m)	—	—	18.9 (Appendix A)
μ_S (N/m)	—	—	18.3 (Appendix A)
$1/q$ (nm)	0	0.18 (Appendix B)	—
CTE (10^{-6}/K)	0.5	17	—

Here I_1 and K_1 are the modified Bessel functions of the first and second kind of order 1. The terms $a-h$ are constants to be determined from the boundary conditions (see the next section, where these constants will be determined after appropriate coupling with interface effects from Sec. II A).

C. Scaling of mechanical stresses: Combination of interfacial and nonlocal effects

Clearly, both the physical mechanisms in Secs. II A and II B must be suitably combined. A careful examination of the main equations in both formulations indicates that the simplest approach would be to adopt the nonlocal solution [Eq. (12)] albeit with one modification at the interconnect-passivation interface: instead of satisfying the normal traction continuity condition, the boundary condition embodied in Eqs. (3) must be satisfied. Although closed-form expressions can be derived for this problem, they are fairly tedious. From a computational point of view, the most efficient procedure is to simply solve for the constants $a-h$ numerically using the boundary conditions given in matrix form in Appendix C. The matrix formulation for the evaluation of the necessary constants, in Appendix C, correctly incorporates the surface elasticity effect derived in Sec. II A. The stress state, as embodied by Eq. (12) and the necessary constants (evaluated in Appendix C) is size dependent due to both interfacial energy effects as well as nonlocal interactions. Thus the scaling of stresses valid for nanointerconnects has been achieved.

III. NUMERICAL RESULTS, DISCUSSION, AND LIMITATIONS

As in several previous works, for the purposes of numerical simulations we assume a copper interconnect embedded within a SiO_2 passivation. All material properties used in the numerical simulations are listed in Table I. We need to determine three surface elastic constants as well as the strain gradient length parameter. The procedure for the former is discussed in Appendix A while the latter is covered in Appendix B. A fairly typical temperature excursion of $-375\,^{\circ}C$ is adopted from the stress-free state.

The (radial) stress in the interconnect, as obtained from the classical formulation[4,5] and the present work, is plotted as a function of the interconnect size in Fig. 3. To separate out the two size effects in our model, the nonlocal effect alone and the interface effect alone are also plotted in Fig. 3.

As expected, the classical stresses do not change as interconnect size is reduced. The nonlocal solution, while indeed showing a size effect, is relatively small. For example, for an interconnect size of 20 nm, the nonlocal effect results in only a 5.7% decrease in the stress. In contrast, the interface effects are substantial, leading to a 32% reduction at 20 nm interconnect size (and 62% if the current technology is ever advanced to 10 nm). Since the interfacial effects appear to be more important, in Fig. 4 we attempt to distinguish between the interfacial tension (τ_0) and the surface elasticity effect (K^S). This is necessary since we have more confidence in the numerical value of τ_0 (known from experiments[30]) while our determination of K^S is highly approximate. Thus in Fig. 4 we plot our solution with surface effects only (ignoring the gradient part) with separate curves representing the interfacial tension effect and the interfacial elasticity effect.

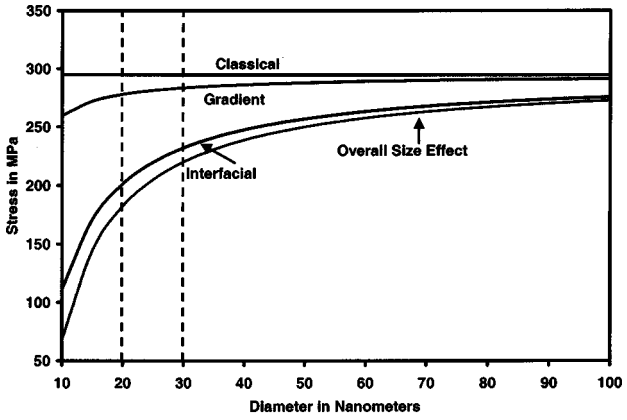

FIG. 3. Stress in the interconnect as a function of interconnect diameter.

Interestingly, the residual tension is the dominant effect (although the impact of K^S is not small either). Even if the term K^S is ignored altogether, the reduction in stresses for an interconnect size of 20 nm is significant ($\sim$39%). Another interesting feature is that K^S acts in an opposite sense to τ_0 as far as stresses are concerned. This is not the case with the strain (where both act in tandem). This is due to the fact that for stress calculation one subtracts the eigenstrain from the actual strain before employing the elastic constitutive law, thus causing K^S to increase the stress (for an eigenstrain that is negative).

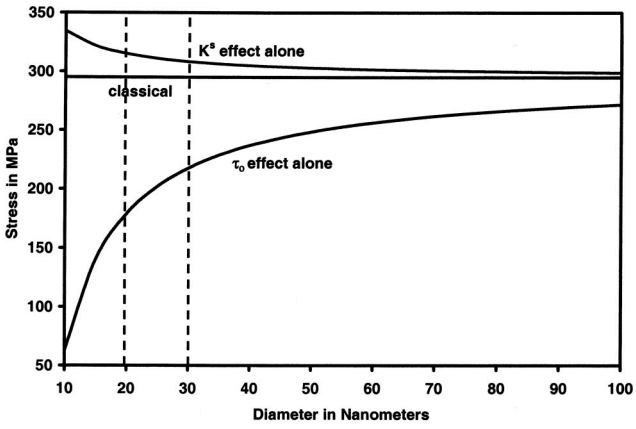

FIG. 4. Separation of K^S and τ_0 effects.

The crucial aspect of these results though is that the reduction of interconnect size to the nanoscale appears to be *beneficial* insofar as mechanical stresses are concerned. The reader should be cautioned against extrapolating this observation to the *reliability* of nanointerconnects. While we can certainly conclude from this study that mechanical stresses are reduced at small length scale, other aspects that govern interconnect reliability must be coaddressed to make stronger claims regarding the reliability of nanointerconnects. Further, needless to say, these results are valid only for the material system we have chosen. Changes in the materials will most likely alter the numerical values although we expect similar qualitative behavior for other systems as well.

IV. SUMMARY

In closure, we have presented scaling laws for mechanical stresses that are applicable to nanointerconnects. Although a simple representative geometry for the interconnect was employed, our conclusions are fairly general. It appears that interfacial effects are fairly appreciable for the nanointerconnect sizes projected by various semiconductor technology roadmaps. In contrast, nonlocal size effects are negligible. The main outcome of the work (apart from the formal development of the associated models) is that stresses appear to be reduced significantly at small length scales as compared to interconnects in the greater than 65 nm regime. Although this reduction is likely to have an important (beneficial) impact on nanointerconnect reliability, more definitive conclusions can be drawn only after establishment of appropriate scaling laws for electromigration, void growth and coalescence, and (of course) incorporation of the present work.

ACKNOWLEDGMENTS

Helpful comments and suggestions from Dr. Deepali Bhate and Dr. Juan Sabate are acknowledged. Partial support from Electronics and Photonics Systems Technology and the Nano Advanced Technology Program is appreciated.

APPENDIX A: DETERMINATION OF CONSTANTS FOR SURFACE ELASTICITY

The experimental determination of the surface/interface constants is nontrivial (even the residual tension τ_0). Most experimental measurements typically report only τ_0 and the surface/interface elasticity parameters are mostly unknown experimentally. Ibach[20] provides a good overview of this subject. A few authors have determined these values using molecular dynamics simulations (see, for example, Ganti *et al.*[31] or Miller and Shenoy[32]). While τ_0 for our material system (Cu-SiO_2) is known from experimental measurements of Cui *et al.*,[30] we determine (approximately) the interfacial elasticity constants using Gurtin and Murdoch's[19] analogy to the membrane theory of Tiersten.[33] A transition from bulk constants to interface/surface properties can be made by the following transformation:

$$\{\mu_S, \lambda_S\} \rightarrow \{\mu h, 2\lambda\mu h/(\lambda+\mu)\}. \tag{A1}$$

Here, h is the thickness over which surface/interface elasticity behavior differs from the bulk. Our molecular dynamics simulations indicate[31] that such behavior is typically confined to about 1–2 lattice spacings. For the interface, we have assumed this value to be 5 Å. The transformation in Eq. (A1) for the Cu-SiO_2 interface is based on their averaged properties.

APPENDIX B: DETERMINATION OF NONLOCAL CONSTANT

Nonlocal material constants represent spatial dispersion that is typically observed in phonon dispersion curves. The classical theory of elasticity predicts no dispersion (i.e., the relation between acoustic frequency and wave number is linearly proportional). In the nonlocal theory framework, however, the acoustic frequency (and hence velocity) becomes wavelength dependent and measures the nonlinear departure of the phonon dispersion curve from the linear prediction of classical elasticity. This allows one to determine the material constant d in Eq. (12). See, for example, Krumhansl,[22] Reid and Gooding,[28] and Eringen.[26] When $\omega^2 = a_1 k^2 + a_2 k^4$ is fitted to the phonon dispersion curve of a solid, $1/q^2$ is given by a_2/a_1. Here ω is the acoustic frequency while k is the wave number. Note that a_1 characterizes the classical constants (i.e., linear frequency/wave number relation) while the dispersion or nonlinearity is measured by a_2. This polynomial form is chosen solely for convenience. For example, from a physical point of view (in the case of a simple linear atomic chain), the relation is transcended in nature. Another method (also by fitting to phonon dispersion curves) is that due to Eringen.[26] The phonon dispersion curves for Cu were taken from Vyas *et al.*[34] while the nonlocal parameter of SiO_2 was assumed to be close to zero (due to its amorphous nature). The gradient length scale $(1/q)$ can often (for most metals) be well approximated by $a_0/2$ (where a_0 is the lattice parameter).

APPENDIX C: DETERMINATION OF BOUNDARY CONDITIONS FOR COMBINED SURFACE ELASTICITY AND NONLOCAL INTERACTIONS

If one were to consider nonlocal interactions alone, Reid and Gooding[28] have discussed the appropriate boundary conditions for a gradient formulation. They discuss the boundary conditions from a variational point of view. Here we discuss them from the point of view of physics while incorporating the effect of surface energies (Sec. II A) also. (1) Displacements must be bounded at the origin. (2) Displacements must be continuous at the interface. (3) Displacements must be zero far away from the interconnect (assuming, like Niwa *et al.*,[5] that the amount of passivation is ''large'' compared to the interconnect). (4) The jump in normal tractions must be balanced by the interfacial stress (consisting of the interfacial tension and the interfacial elasticity term weighted appropriately by the interconnect size). (5) The gradients of the strain must be continuous across the interface. (6) There must be higher-order gradient continuity. Based on conditions 1 and 3, the constants b, d, e, and g must be set to zero. The

remaining four constants (a, c, f, and h) are determined based on conditions 2, 4, 5, and 6. In matrix form, we can write them as follows:

$$\begin{bmatrix} q_I R_0 & I_1(q_I R_0) & -\frac{1}{q_P R_0} & -K_1(q_P R_0) \\ q_I & q_I I_1'(q_I R_0) & \frac{1}{q_P R_0^2} & -q_P K_1'(q_P R_0) \\ 0 & d_I q_I^2 I_1''(q_I R_0) & \frac{-2d_P}{q_P R_0^3} & -d_P q_P^2 K_1''(q_P R_0) \\ \alpha_1 & \alpha_2 & \beta_1 & \beta_2 \end{bmatrix} \times \begin{bmatrix} a \\ c \\ f \\ h \end{bmatrix} = \begin{bmatrix} 0 \\ 0 \\ 0 \\ 2(\lambda_I+\mu_I)\varepsilon^* R_0 - \tau_0 \end{bmatrix}, \tag{C1}$$

where

$$\alpha_1 = (\lambda_I+2\mu_I) q_I R_0 + \left(\lambda_I - \frac{6d_I}{R_0^2}\right) q_I R_0 + \frac{6d_I}{R_0} q_I + \left(\frac{2\mu_S+\lambda_S}{R_0}\right) q_I R_0,$$

$$\alpha_2 = \left(\lambda_I - \frac{6d_I}{R_0^2}\right) I_1(q_I R_0) + (\lambda_I+2\mu_I) q_I R_0 I_1'(q_I R_0) + \frac{6d_I}{R_0} q_I I_1'(q_I R_0) - 2d_I q_I^2 I_1''(q_I R_0) - 2d_I R_0 q_I^3 I_1'''(q_I R_0) + \left(\frac{2\mu_S+\lambda_S}{R_0}\right) I_1(q_I R_0),$$

$$\beta_1 = \frac{(\lambda_P+2\mu_P)}{q_P R_0} - \frac{(\lambda_P - 6d_P/R_0^2)}{q_P R_0} - \frac{2d_P}{q_P R_0^3},$$

$$\beta_2 = -(\lambda_P+2\mu_P) q_P R_0 K_1' - \left(\lambda_P - \frac{6d_P}{R_0^2}\right) K_1 - \frac{6d_P}{R_0} q_P K_1' + 2d_P q_P^2 K_1'' + 2d_P R_0 q_P^3 K_1'''.$$

[1] A. Wikstrom, P. Gudmundson, and S. Suresh, J. Appl. Phys. **86**, 6088 (1999).
[2] A. Gouldstone, Y.-L. Shen, S. Suresh, and C. V. Thompson, J. Mater. Res. **13**, 1956 (1998).
[3] A. I. Sauter and W. D. Nix, IEEE Trans. Compon., Hybrids, Manuf. Technol. **15**, 594 (1992).
[4] M. A. Korhonen, R. D. Black, and C.-Y. Li, J. Appl. Phys. **69**, 1748 (1991).
[5] H. Niwa, H. Yagi, H. Tsuchikawa, and M. Kato, J. Appl. Phys. **68**, 328 (1990).
[6] P. Sharma, H. Ardebili, and J. Loman, Appl. Phys. Lett. **79**, 1706 (2001).
[7] C. H. Hsueh, J. Appl. Phys. **92**, 144 (2002).
[8] D. N. Bhate, A. Kumar, and A. F. Bower, J. Appl. Phys. **87**, 1712 (2000).
[9] *Materials Reliability in Microelectronics IV*, edited by P. Borgensen *et al.* (Materials Research Society, Pittsburgh, PA, 1994).
[10] ITRS (International Technical Roadmap for Semiconductors) roadmap for interconnect technology, 2001.
[11] *Quantum Dots and Nanowires*, edited by S. Bandyopadhyay and H. S. Nalwa (American Scientific Publishers, Stevenson Ranch, CA, 2003).
[12] J. D. Meindl, Comput. Sci. Eng. **5**, 20 (2003).
[13] A. E. Kaloyeros, E. T. Elsenbraun, J. Welch, and R. E. Geer, Semicond. Int. **26**, 56 (2003).
[14] X. Pang, A. M. Kriman, and G. H. Bernstein, J. Electrochem. Soc. **149**, G103 (2002).
[15] M. Kato, H. Niwa, H. Yagi, and H. Tsuchikawa, J. Appl. Phys. **68**, 334 (1990).
[16] J. D. Eshelby, Proc. R. Soc. London, Ser. A **241**, 376 (1957).
[17] M. E. Gurtin, J. Weissmuller, and F. Larche, Philos. Mag. A **78**, 1093 (1998).
[18] M. E. Gurtin and A. I. Murdoch, Arch. Ration. Mech. Anal. **59**, 389 (1975).
[19] M. E. Gurtin and A. I. Murdoch, Int. J. Solids Struct. **14**, 431 (1978).
[20] H. Ibach, Surf. Sci. Rep. **29**, 193 (1997).
[21] P. Sharma and S. Ganti (unpublished).
[22] J. A. Krumhansl, in *Mechanics of Generalized Continua*, edited by E. Kroner (Springer-Verlag, Berlin, 1968), p. 298.
[23] I. A. Kunin, Prikl. Mat. Mekh. **30**, 542 (1966).
[24] A. C. Eringen and D. G. B. Edelen, Int. J. Eng. Sci. **10**, 233 (1972).
[25] I. A. Kunin, *Elastic Media with Microstructure I* (Springer-Verlag, Berlin, 1982).
[26] I. A. Kunin, *Elastic Media with Microstructure II* (Springer-Verlag, Berlin, 1983).
[27] A. C. Eringen, *Nonlocal Continuum Field Theories* (Springer-Verlag, New York, 2002).
[28] A. C. E. Reid and R. J. Gooding, Phys. Rev. B **46**, 6045 (1992).
[29] P. Sharma and S. Ganti, Philos. Mag. Lett. (to be published).
[30] G. Cui, M. Lane, K. Vijayamohanan, and G. Ramanath, Mater. Res. Soc. Symp. Proc. **695**, 329 (2002).
[31] S. Ganti, P. Sharma, and N. Bhate (unpublished).
[32] R. E. Miller and V. B. Shenoy, Nanotechnology **11**, 139 (2000).
[33] H. F. Tiersten, J. Appl. Phys. **40**, 770 (1969).
[34] P. R. Vyas, C. V. Pandya, T. C. Pandya, and V. B. Gohel, Pramana, J. Phys. **56**, 559 (2001).